


PRIMARY RESEARCH

Open Access



Tetraspanin 7 promotes osteosarcoma cell invasion and metastasis by inducing EMT and activating the FAK-Src-Ras-ERK1/2 signaling pathway

Shijie Shao^{1†}, Lianhua Piao^{2*†}, Liwei Guo¹, Jiansong Wang¹, Luhui Wang¹, Jiawen Wang¹, Lei Tong¹, Xiaofeng Yuan¹, Junke Zhu¹, Sheng Fang¹ and Yimin Wang^{1*} 

Abstract

Background: Tetraspanins are members of the 4-transmembrane protein superfamily (TM4SF) that function by recruiting many cell surface receptors and signaling proteins into tetraspanin-enriched microdomains (TEMs) that play vital roles in the regulation of key cellular processes including adhesion, motility, and proliferation. Tetraspanin7 (Tspan7) is a member of this superfamily that plays documented roles in hippocampal neurogenesis, synaptic transmission, and malignant transformation in certain tumor types. How Tspan7 influences the onset or progression of osteosarcoma (OS), however, remains to be defined. Herein, this study aimed to explore the relationship between Tspan7 and the malignant progression of OS, and its underlying mechanism of action.

Methods: In this study, the levels of Tspan7 expression in human OS cell lines were evaluated via qRT-PCR and western blotting. The effect of Tspan7 on proliferation was examined using CCK-8 and colony formation assays, while metastatic role of Tspan7 was assessed by functional assays both in vitro and in vivo. In addition, mass spectrometry and co-immunoprecipitation were performed to verify the interaction between Tspan7 and $\beta 1$ integrin, and western blotting was used to explore the mechanisms of Tspan7 in OS progresses.

Results: We found that Tspan7 is highly expressed in primary OS tumors and OS cell lines. Downregulation of Tspan7 significantly suppressed OS growth, metastasis, and attenuated epithelial-mesenchymal transition (EMT), while its overexpression had the opposite effects in vitro. Furthermore, it exhibited reduced OS pulmonary metastases in Tspan7-deleted mice comparing control mice in vivo. Additionally, we proved that Tspan7 interacted with $\beta 1$ integrin to facilitate OS metastasis through the activation of integrin-mediated downstream FAK-Src-Ras-ERK1/2 signaling pathway.

Conclusion: In summary, this study demonstrates for the first time that Tspan7 promotes OS metastasis via interacting with $\beta 1$ integrin and activating the FAK-Src-Ras-ERK1/2 pathway, which could provide rationale for a new therapeutic strategy for OS.

*Correspondence: piaolianhua@jsut.edu.cn; wangyimin1515@suda.edu.cn

[†]Shijie Shao and Lianhua Piao equally contributed to this work

¹ Department of Orthopedics, The Third Affiliated Hospital of Soochow University, Changzhou 213000, People's Republic of China

² Institute of Bioinformatics and Medical Engineering, Jiangsu University of Technology, Changzhou 213000, People's Republic of China



Keywords: Tspan7, Osteosarcoma, Integrin $\beta 1$, EMT, FAK-Src-Ras-ERK1/2 signaling pathway

Background

Osteosarcoma (OS) is one of the commonest prevalent form of bone malignancy, arising from immature bone stromal spindle cells and primarily affecting the epiphysis regions of long bones in children and adolescents [1], with an estimated annual incidence of OS is 3/1,000,000 [2]. Historically, patients diagnosed with OS before the 1970s exhibited a poor 5 year survival rate of just 15% owing to amputation being the only available treatment option [3], although these rates have risen to 60–70% with the advent of neoadjuvant chemotherapeutic drugs including cisplatin, doxorubicin, and methotrexate [4]. However, many patients still succumb to this disease in large part owing to the rapidity with which it progresses and metastasizes, with the lungs being the most common site of distant OS tumor metastasis. The further refinement of surgical approaches and neoadjuvant chemotherapy regimens have not significantly improved the survival of OS patients. As such, there is a clear need for further studies exploring relevant molecular targets associated with the mechanistic basis for OS metastatic progression.

Tetraspanins are members of the four-transmembrane protein superfamily (TM4SF) of which 33 have been identified to date in mammals, exhibiting diverse tissue- and organ-specific expression patterns [5]. All tetraspanins exhibit a high degree of structural homology including four transmembrane domains (TM1-4), a large extracellular loop (LEL) and a small extracellular loop (SEL), as well as a small intracellular loop [6]. In functional contexts, tetraspanins bring together a variety of membrane and cytosolic proteins such as integrins, kinases, and receptors within cells in clusters known as tetraspanin-enriched microdomains (TEMs) that orchestrate downstream signaling to regulate proliferation, migration, differentiation, and adhesion in both physiological and pathological contexts such as tumor cell metastasis [7, 8]. The epithelial-mesenchymal transition (EMT) is a key process whereby tumor cells acquire a more migratory and aggressive phenotype conducive to metastasis. Several studies have highlighted roles for tetraspanins in the induction or regulation of this EMT process. For example, one recent analysis demonstrated that non-small cell lung cancer (NSCLC) cells overexpressing tetraspanin7 (Tspan7) exhibited enhanced migratory activity attributable to more robust EMT induction [9]. In contrast, CD82 (Tspan27) inhibits fibronectin-induced EMT progression by interacting with the $\alpha 3\beta 1/\alpha 5\beta 1$ integrins which form the fibronectin receptor to disrupt

downstream focal adhesion kinase (FAK)/Src and ILK pathway activation [10]. Other members of TM4SF family including Tspan8, CD63, and CD151 have also been proved to regulate key steps in EMT in either an oncogenic or tumor suppressor capacity in cancers such as melanoma, colorectal cancer, and renal cell carcinoma [11–13]. In light of their structural homologies and the above evidence, we hypothesized that Tspan7 may serve as an important EMT regulator in multiple cancer types. Integrins are α/β heterodimeric adhesion receptors capable of binding to specific molecules within the extracellular matrix (ECM) and on cell surfaces, particularly tetraspanins, and thereupon activating a range of signaling pathways including the FAK pathway to modulate cellular proliferation, survival, migration, and EMT induction [14–16]. Many different integrin heterodimers including $\alpha 3\beta 1$, $\alpha 4\beta 1$, $\alpha 6\beta 1$, and $\alpha v\beta 3$ have been shown to interact with TM4SF proteins including Tspan1, CD9, CD53, CD63, CD81, and CD82 in the context of oncogenesis [17–19]. Currently, it remains poorly understood whether Tspan7 is able to interact with specific integrin partners to regulate tumor progression.

Tspan7 (also known as TM4SF2, CD231, and A15) is encoded on chromosome Xp11.4 in humans and is expressed at high levels by non-hematopoietic cells, with pronounced expression being evident in the hippocampal and cerebral cortex regions of the brain [20, 21]. This protein plays a vital role in normal synaptic transmission and the development of hippocampal neurons [22], with Tspan7 mutations having been linked to intellectual disabilities including X-linked mental retardation [23]. Autoantibodies specific for Tspan7 can also aid in the identification of adults with type 1 diabetes mellitus, and may offer value for the immunotherapeutic treatment of certain latent forms of this autoimmune condition [24, 25]. Furthermore, Tspan7 has been identified as a promising biomarker and functional regulatory protein associated with several cancers such as multiple myeloma [26], clear-cell renal cell carcinoma [27], head and neck squamous cell carcinoma [28], primary uterine leiomyosarcoma [29], and desmoplastic small round-cell tumors [30]. The complex roles played by this tetraspanin have been explored at length in certain oncogenic settings. For example, the overexpression of Tspan7 in liver cancer and multiple myeloma cells markedly enhances their metastatic potential [26, 31], whereas exerts an anti-tumor effects in bladder tumors and suppresses the growth of cancer cell through the PTEN/PI3K/Akt signaling pathway [32]. Wang et al. [9] found that in NSCLC,

Tspan7 plays a pro-oncogenic role. As such, Tspan7 may play pro- or anti-tumorigenic roles in a context-dependent manner. Notably, nevertheless, no studies have clearly explored the effect of Tspan7 in OS progression.

Consequently, we explored the expression of Tspan7 in OS cell lines and tumor tissue samples and found it to be elevated therein relative to corresponding controls. Knocking down Tspan7 was sufficient to suppress the proliferation of OS cancer cells. We thus explored the functional impact of Tspan7 expression on the metastatic progression of OS tumors both in vitro and in vivo, revealing that it contributes to tumor cell migratory activity through both the induction of EMT and the interaction with $\beta 1$ integrin that ultimately results in the activation of FAK-Src-Ras-ERK1/2 pathway. Together, these results offer new insights regarding the mechanistic basis of Tspan7 for OS onset and progression, and they further highlight Tspan7 as a promising therapeutic target in the management of patients with OS.

Materials and methods

Microarray data collection and analysis

OS-related gene expression data were retrieved from the Gene Expression Omnibus (GEO) database (<http://www.ncbi.nlm.nih.gov/geo>) from datasets with the following accession numbers: GSE14359 [including 18 primary OS tissue samples and 2 normal osteoblast (OB) samples], GSE12865 (including 12 OS tissue samples and 2 OB samples), GSE33383 [including 84 OS tissue samples, 3 OB samples, and 12 normal mesenchymal stem cell (MSC) samples], and GSE42352 (including 19 primary OS cell lines, 3 OB samples, and 12 MSC samples).

Cell culture and transfection

HEK293T, HOS, Saos2, Mg63, and U2OS cells (Chinese Academy of Cell Resource Center) were cultivated in DMEM/MEM (Gibco, CA, USA) supplemented with 10% FBS (ScienCell, CA, USA) in a humid incubator under 37 °C and 5% CO₂.

Tspan7 knockdown was achieved by synthesizing two siRNA duplexes specific for this tetraspanin (siTspan7#1 and siTspan7#2) or a corresponding negative control (siNC) construct (Biolino Nucleic Acid Technology Co., Ltd). HOS cells were transfected with appropriate siNC or siTspan7 constructs (100 nM) utilizing Lipofectamine[®] RNAiMAX (Thermo Fisher Scientific, Inc.) based upon provided directions.

U2OS cells stably expressing the OE-Tspan7 or mock constructs were treated with Ras inhibitor (Salirasib; #HY-14754; 50 μ M) for 48 h, and then either assessed with respect to their migratory and invasive activities or protein expression via western blotting.

CCK-8 kit (Dojindo Molecular Technologies, Inc., China) was utilized to assess cellular viability. For colony formation assays, HOS cells were cultured in 6-well plates and treated with appropriate siRNA constructs (5000/well). Cells were then incubated for 10–14 days, after which colonies were fixed using methanol and stained using 0.1% crystal violet. Experiments were repeated in triplicate.

qRT-PCR

The MiniBEST Universal RNA Extraction kit (Takara, Dalian, China) and the first-strand cDNA Synthesis Kit (Takara) was used to obtain the cDNA from cell lines. All qRT-PCR reactions were prepared with a SYBR Premix Ex Taq kit (Takara) and run under the following settings: 95 °C for 30 s; 40 cycles of 95 °C for 5 s, 60 °C for 30 s in StepOnePlus RT-PCR instrument (Applied Biosystems, Shanghai, China). The relative gene expression was assessed via the $2^{-\Delta\Delta C_q}$ method, with GAPDH as a normalization control. All primers and siRNA sequences used herein are listed in Table 1.

Plasmid transfection

Tspan7-specific short hairpin RNAs (shTspan7#1, shTspan7#2) and a corresponding negative control (shNC) were inserted into the LV-3 (pGLVH1/GFP + Puro) vector (GenePharma, Shanghai, China). Lipofectamine 3000 was then used to transfect these plasmids into HEK293T cells based on the provided directions. After 24 h, the supernatants including lentiviral particles were collected and used to transduce HOS and Saos2 cells (40–70% confluent) in the presence of polybrene (8 μ g/mL).

Table 1 The primers and siRNA/shRNA sequences used in this study

Name		Sequences
Tspan7	Forward	GCTGCATGAACGAAACTGATTG
	Reverse	GGCGGCCACAGTCAGATT
GAPDH	Forward	ATGGAAATCCCATCACCATCTT
	Reverse	CGCCCCACTTGATTTTGG
Tspan7 siRNAs		
	siTspan7#1	Sense GCGAGACUUACA AUGGCAAUTT Antisense AUUGCCAUUGUAAGUCUGCTT
siTspan7#2	Sense	GGUUGUUUAUGAUCUGGUAATT
	Antisense	UUACCAGAUAUAACAACCTT
Negative control (siNC)	Sense	UUCUCCGAACGUGUCACGUTT
	Antisense	ACGUGACACGUUCGGAGAATT
Tspan7 shRNAs		
	shTspan7#1	5'-3' GTTTGTATGATCTGGTAA
shTspan7#2	5'-3' GCACCTATATCTCCCTTAT	
Negative control (shNC)	5'-3' TTCTCCGAACGTGTCACGT	

Puromycin (2 mg/mL) was used to select for cells stably deleted Tspan7.

The FLAG-tagged Tspan7 expression vector was cloned, and used to prepare lentiviral particles as above. U2OS cells were then transduced with the resultant lentiviral particles, and blasticidin (2 mg/mL) was used to select for the stably transformed cells. Western blotting and qRT-PCR were used to confirm knockdown or over-expression of Tspan7. The shRNA sequences employed in this research were compiled in Table 1.

RNA-sequencing

RNA-seq analyses were conducted with an Illumina HiSeq 2000 instrument (Illumina, Inc., USA). Briefly, total RNA isolated from HOS cells expressing shNC or shTspan7 was collected, and the integrity thereof was confirmed with an Agilent Bioanalyzer 2100 instrument (Agilent Technologies, Inc., USA). Following sequencing, genes that were significantly differentially expressed were identified (fold change ≥ 2 and $P < 0.05$), and pathway analyses of these differentially expressed genes (DEGs) were conducted using the Gene Ontology (GO) (<http://www.geneontology.org>) and Kyoto Encyclopedia of Genes and Genomes (KEGG) database (<https://www.genome.jp/kegg>) tools.

Wound healing and transwell assays

Wound healing assays were employed to assess the migratory ability of OS cells. When cells were 90–100% confluent, a sterile micropipette tip was used to generate a scratch wound in the monolayer surface. Cells were cultured in serum-free media, with the wound being imaged via light microscope after 0, 24, and 48 h. The ImageJ software was used to measure the wound area in 10 random fields of view, and the percentage of wound closure was calculated using the following formula: $[1 - (\text{wound area at 24 h or 48 h} / \text{wound area at 0 h})] \times 100\%$.

Transwell filter inserts (#3464, Corning, USA) were additionally used to assess OS cell migration activity. Briefly, 2×10^4 cells in 150 μL of serum-free media were added to the upper chambers of the Transwell inserts in 24-well plates with 600 μL of media containing 10% FBS. After incubating 16–18 h, cells were rinsed with PBS, fixed using methanol, stained with crystal violet for 1 h, and the migratory cells were then measured after gently removing cells from the inner surface of the inserts with a cotton swab. For invasion assays, with 1×10^5 of cells in 500 μL serum-free media being added to the upper portion of Matrigel invasion chambers (#354,480, BD, USA) that were placed into 24-well plates containing 700 μL of complete media per well. Following an 18–20 h incubation, a cotton swab was used to remove non-invasive cells, while the remaining cells were fixed using methanol

and stained for 1 h with crystal violet. All migratory and invasive cells in six random fields of view per sample were counted with a light microscope, and all the experiments were conducted in triplicate.

Western blotting and immunoprecipitation (IP)

RIPA buffer containing a protease inhibitor cocktail (Roche Applied Science, Penzberg, Germany) was used to lyse cells under sonication. The supernatants were collected after a centrifuge and the concentration was quantified using a BCA assay kit (Beyotime Biotechnology, Shanghai, China). Proteins were then separated via SDS-PAGE and transferred onto 0.45 μm PVDF membranes (Millipore, USA). Blots were blocked with 5% non-fat milk in TBST, and were then incubated overnight at 4 °C with the antibodies specific for the following: Tspan7 (1:300, #A13555, ABclonal), FN1 (1:1000, #A12932, ABclonal), N-Cadherin (1:1000, #13,116, CST), Vimentin (1:1000, #5741, CST), Slug (1:1000, #9585, CST), Snai1 (1:1000, #3879, CST), phospho-FAK^{Y397} (1:500, #ab81298, Abcam), phospho-FAK^{Y925} (1:500, #3284 T, CST), total-FAK (1:1000, #ab40794, Abcam), phospho-Src^{Y529} (1:500, #AP0185, ABclonal), total-Src (1:500, #A19119, ABclonal), Ras (1:1000, #ab52939, Abcam), phospho-ERK1/2 (1:1000, #4370, CST), total-ERK1/2 (1:1000, #4695, CST), integrin $\beta 1$ /ITGB1 (1:500, #A2217, ABclonal), Flag (1:1000, #F7425, Sigma), and β -actin (1:1000, #A5441, Sigma-Aldrich). Primary antibody dilution buffer (#P0256, Beyotime Biotechnology, China) was used to prepare all antibodies. U2OS cells expressing FLAG-tagged Tspan7 or control constructs were grown in 10 cm dishes. Anti-Flag M2 agarose beads (#A2220, Sigma) were used to purify Flag-tagged Tspan7 proteins. Precipitates were then rinsed thrice with PBS, boiled in sample loading buffer, separated via SDS-PAGE, and analyzed via western blotting as above. Proteins interacting with Tspan7 as identified by mass spectrometry.

Animals experiments

5–6 weeks old female nude mice from Qinglong Mountain Animal Breeding Center (Nanjing, China) were housed under controlled conditions (18–23 °C, 12 h light/dark cycle) with free food and water access. Briefly, a model of OS cell lung metastasis was established by injecting mice with 2×10^6 HOS cells (shNC or shTspan7#2) in sterile PBS via the lateral tail vein. Four weeks later, lungs were resected, fixed using 4% formaldehyde for 24 h, and metastatic nodules visible on the lung surface were counted. Samples were then paraffin-embedded, cut into 5 μm sections, and subjected to hematoxylin and eosin (H&E) staining. Prepared sections were imaged using a microscopy (magnification, 5 \times and 10 \times). Euthanasia was performed with an intravenous

injection of 150 mg/kg of pentobarbital sodium. The Animal Care Committee of the Third Affiliated Hospital of Soochow University approved this animal study, which was performed in a manner consistent with institutional care guidelines.

Statistical analysis

Data were analyzed using SPSS v21.0 (IBM Corp., NY, USA). The qRT-PCR data were presented as the mean \pm standard error of the mean, and the other data were presented as the mean \pm standard deviation, with $P < 0.05$ as the significance threshold.

Results

Human OS tumor tissues and cell lines exhibit Tspan7 upregulation

To assess patterns of Tspan7 expression in OS, we evaluated the microarray data available through the GEO database, revealing Tspan7 to be significantly upregulated in OS tissues relative to OBs in the GSE14359 ($P = 0.0031$, fold change = 11.9436) and GSE12865 ($P = 0.0048$, fold change = 8.3701) datasets (Fig. 1A, B). According to the GSE33383 dataset, it was upregulated in OS tissues compared to normal MSCs ($P = 0.0001$, fold change = 2.6007) and OBs ($P = 0.0079$, fold change = 2.6563) (Fig. 1C). Consistent with these results, Tspan7 was also expressed at higher levels in OS cell lines as compared with MSCs ($P = 0.0039$, fold change = 1.4743) according to the GSE42353 dataset (Fig. 1D). To confirm these results, Tspan7 mRNA and protein expression were assessed via qRT-PCR and western blotting in Mg63, HOS, Saos2, and U2OS cell lines (Fig. 1E, F). This analysis revealed Tspan7 to be expressed at notably higher levels in HOS and Saos2 cells, whereas slightly lower in U2OS. Further receiver operating characteristics (ROC) curve analyses from the GSE33383 and GSE42352 datasets revealed Tspan7 to be a valuable biomarker capable of differentiating between healthy and OS tumor tissues and cell lines (Fig. 1G). Tspan7 has previously been shown to play either pro- or anti-oncogenic roles in different cancer types. The above data, however, suggests that Tspan7 expression is enhanced in OS, highlighting a likely role for this tetraspanin in OS onset and/or progression.

Tspan7 silencing impairs OS cell viability

Given that HOS cells exhibited higher levels of Tspan7 expression relative to other cell lines, we next knocked down this tetraspanin in HOS cells using two siRNA constructs (siTspan7#1 or siTspan7#2), confirming successful knockdown relative to siNC transfection via qRT-PCR (Fig. 2A). In a CCK-8 assay conducted at 72 h post-transfection, we found that the silencing of Tspan7 led to a significant decrease in HOS cell viability relative to siNC

(Fig. 2B). Consistently, in a colony formation assay we observed significantly fewer, smaller colonies in siTspan7 groups on day 12 post-transfection as compared to the control group (Fig. 2C). Together, these data suggested that the knockdown of Tspan7 was sufficient to impair OS cell proliferation, implying a potential role for this protein in the context of OS progression.

Downstream genes of Tspan7 were identified by RNA-seq analysis

To better understand the functional roles of Tspan7 as an adjuster of OS development and progression, we next performed RNA-seq analysis aimed at identifying differentially expressed genes upon Tspan7 knockdown (shTspan7#1 and shTspan7#2) in HOS cells. Using standardized significance criteria (fold-change ≥ 2 and $P < 0.05$), 764 Tspan7-regulated genes were identified by comparing these groups, including 348 down- and 416 up-regulated, respectively (Fig. 2D, E). Of note, fibronectin 1 (FN1), which is a mesenchymal marker associated with EMT induction and cellular adhesion, was markedly reduced in the shTspan7 group relative to the shNC group, suggesting that Tspan7 may positively regulate FN1 (Table 2), and be involved in the EMT process. GO and KEGG pathway enrichment analyses were then conducted to understand the biological roles of Tspan7-related DEGs at a $P < 0.05$ cutoff threshold. Enriched GO terms indicated that Tspan7 was associated with the regulation of developmental growth (GO: 0,048,638), positive regulation of cell adhesion (GO: 0,045,785), regulation of ERK1 and ERK2 cascade (GO: 0,070,372), and the activation of protein kinase activity (GO: 0,032,147) (Fig. 2F). KEGG pathway enrichment analyses similarly revealed these DEGs to be enriched in the MAPK signaling (hsa04010), Oxytocin signaling (hsa04913), and ECM-receptor interaction (hsa04512) pathways (Fig. 2G).

Tspan7 regulates the migration and invasion of OS cells

Several other tetraspanins including CD82 and CD151 have been identified as tumor suppressors or oncogenic in multiple cancer types owing to their ability to regulate tumor cell metastasis [33, 34]. Tspan7-mediated enhancement of EMT induction was recently reported to play a central role in lung cancer metastasis [9]. Upon GO and KEGG analyses, Tspan7 was also likely to be involved in OS cancer cell metastasis. Thus, we attempted to find out the mechanisms how Tspan7 controls the metastatic progression of OS. We stably knocked down Tspan7 in HOS and Saos2 cells using shRNA constructs (shTspan7#1 or shTspan7#2), confirming successful knockdown via qRT-PCR and western blotting (Fig. 3A), as well as fluorescent microscopy (Fig. 3B). In wound healing and Transwell assays, depleting Tspan7 was found to markedly impair

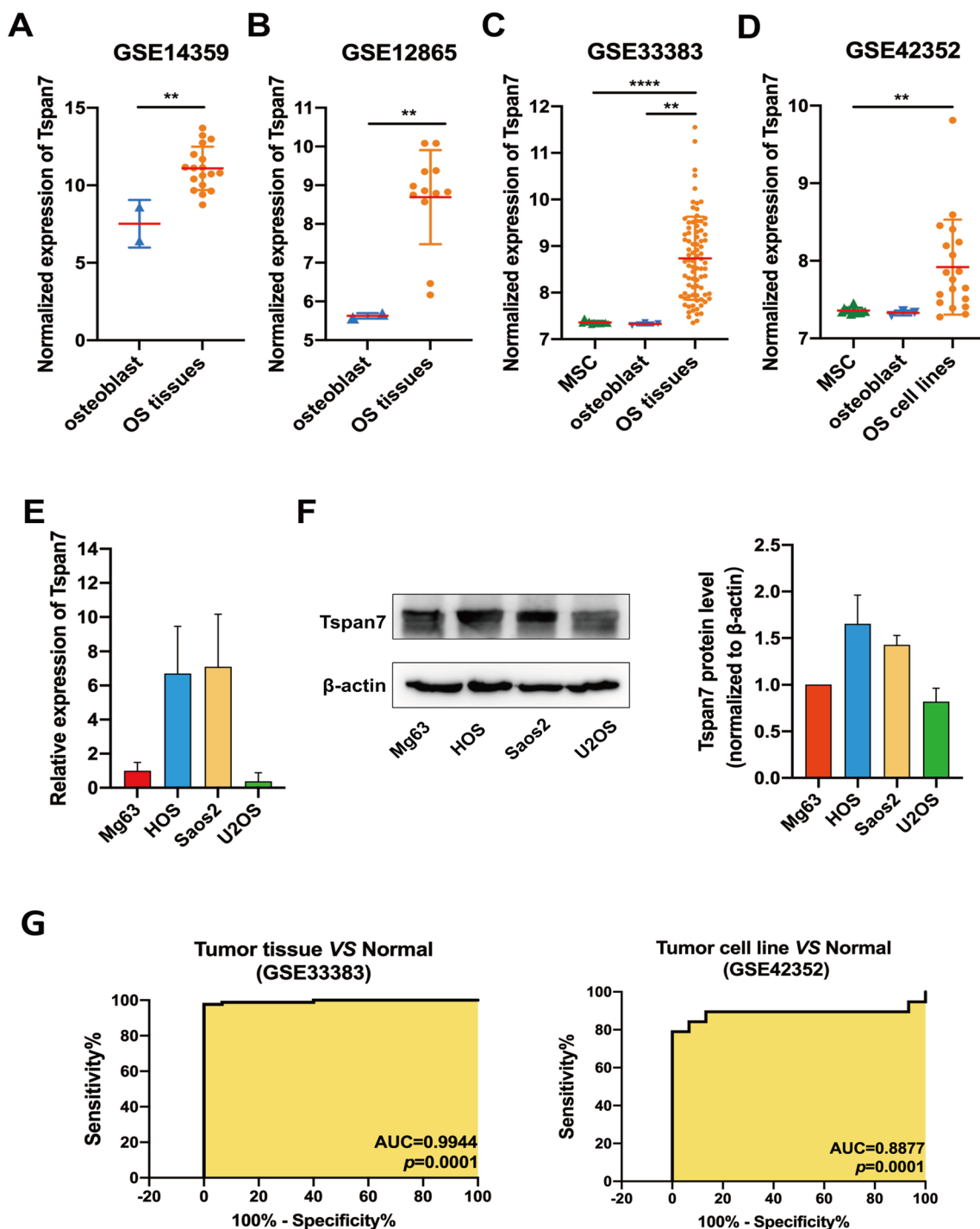


Fig. 1 OS tumor tissues and cell lines exhibit Tspan7 upregulation. **A–D** The mRNA-level expression of Tspan7 was markedly increased in OS tissues and cell lines relative to corresponding normal controls (OBs and MSCs) in the GSE (14,359, 12,865, 33,383, and 42,352) datasets. **E** Relative to Mg63 cells, HOS and Saos2 cells exhibited significantly increased Tspan7 mRNA levels in a qRT-PCR assay, whereas this level was decreased in U2OS cells. GAPDH served as a normalization control. Data are means \pm SEM from two separate experiments. **F** Western blotting results showed that Tspan7 in HOS and Saos2 but not U2OS was markedly higher compared with Mg63 cell. Bands were normalized to the β -actin loading control. Data are presented as the means \pm SD of two independent experiments. **G** ROC curves and AUC values for OS based upon the GSE33383 and GSE42352 dataset. GAPDH, glyceraldehyde-3-phosphate dehydrogenase; ROC, receiver operating characteristic; AUC area under the curve, SD standard deviation. ** $P < 0.01$, **** $P < 0.0001$. Student's t-test

Table 2 Eleven of 232 DEGs enriched in cancer metastasis-related GO processes (regulation of cell adhesion, GO:0,045,785)

Gene names	Expression value – shTspan7#1	Expression value – shTspan7#2	Expression value – shNC#1	Expression value – shNC#2	Log ² fold change	p-value
<i>SIRPB1</i>	1.118376464	0.495721813	0.80962826	2.165084088	– 3.227314657	<i>p</i> < 0.05
<i>PIK3R6</i>	0.340225214	0.62066055	0.633537001	1.715767173	– 3.126669927	<i>p</i> < 0.05
<i>HAS2</i>	0.817346468	0.319630554	1.6547263	1.258389977	– 2.885789675	<i>p</i> < 0.05
FN1	3.418682032	3.319196043	3.551829513	4.296320867	– 2.310111273	<i>p</i> < 0.05
<i>TPM1</i>	3.368796466	3.628408328	4.124010519	3.896079796	– 1.684664957	<i>p</i> < 0.05
<i>FERMT1</i>	1.852108575	2.167819671	2.658842866	2.107604583	– 1.423064871	<i>p</i> < 0.05
<i>IL7R</i>	2.887999919	3.038961841	3.468381406	3.193897243	– 1.271159105	<i>p</i> < 0.05
<i>IGF2</i>	2.672663674	2.782776691	2.829436653	3.270101357	– 1.234961466	<i>p</i> < 0.05
<i>S100A10</i>	3.747871011	3.777285409	3.901958948	4.228364707	– 1.103723422	<i>p</i> < 0.05
<i>PODXL</i>	3.892223833	3.599639507	3.739103952	4.266308368	– 1.023388653	<i>p</i> < 0.05
<i>SDC4</i>	3.623752579	3.443318896	3.570804073	4.017503585	– 1.017531903	<i>p</i> < 0.05

The significance of row given in bold in the table is to highlight the direction of research

the in vitro migration of HOS and Saos2 cells (Fig. 3C, D). Similarly, when Matrigel-coated invasion cells were used to evaluate the invasive activity of OS cells, Tspan7 knockdown was confirmed to suppress such invasive activity (Fig. 3E). To evaluate the impact of Tspan7 overexpression on such migratory and invasive activities, U2OS cells with low endogenous Tspan7 expression were engineered to overexpress this tetraspanin as assessed by qRT-PCR and western blotting, as well as fluorescent microscopy (Fig. 3F). Then, wound healing and Transwell assays revealed that these OE-Tspan7 U2OS cells exhibited markedly enhanced migratory activity as compared to mock control cells (Fig. 3G, H), with concomitant enhancement in invasiveness (Fig. 3I). These findings thus provided robust evidence that Tspan7 can promote the in vitro invasive and migratory potential of OS cells.

Tspan7 downregulation inhibits EMT induction and OS cell metastasis in vivo

Tspan7 was confirmed to be closely associated with cellular adhesion in our GO enrichment analyses. Therefore, in the present study, we next sought to establish a link between Tspan7 and EMT process in the context of OS cell metastasis. Western blotting results showed that

OE-Tspan7 cells exhibited a significantly increased FN1 expression, an EMT biomarker as well as a downstream candidate of Tspan7, relative to control cells (Fig. 4A, B). We further found that the knockdown of Tspan7 in HOS cells caused reductions in interstitial biomarkers (Vimentin and N-cadherin) expression and EMT-related transcription factors (Snai1 and Slug) therein, consistent with the impairment of the EMT process (Fig. 4A, B). Conversely, the overexpression of Tspan7 in U2OS cells was linked to increases in the expression of all four of these EMT-related proteins (Fig. 4A, B). Together, these results suggested that Tspan7 might be able to promote OS cell metastasis via the positive regulation of the EMT process.

To more fully clarify the link between Tspan7 and the metastatic progression of OS in vivo, an OS pulmonary metastasis model was established. Following the injection of tumor cells into the tail vein of mice, only a subset of animals ultimately developed pulmonary metastases at a rate proportional to the overall invasive and metastatic ability of the injected cells. While four animals in the control group developed metastatic lung foci, whereas two in the shTspan7 group. There was a clear reduction in the total number of metastatic nodules in the shRNA

(See figure on next page.)

Fig. 2 Tspan7 knockdown suppresses the proliferation of OS cells; Tspan7-associated biological functions based on RNA-seq analysis. **A** The knockdown of Tspan7 was confirmed via qRT-PCR at 72 h post-transfection in cells transfected with siTspan7 and siNC. **B** The viability of cells transfected with siTspan7 or siNC was assessed via CCK-8 assay at 72 h post-transfection. **C** The effect of Tspan7 silencing on HOS cell growth was assessed in a colony formation assay. Statistical results of colony formation numbers normalized to the NC group were presented. **D** Top DEGs identified following Tspan7 knockdown in HOS cells are arranged in a heatmap, with shNC cells being used for comparison. **E** The 764 DEGs identified when comparing shTspan7 and shNC groups at an adjusted $|\log_2\text{FoldChange}| \geq 1$ and $P < 0.05$ are shown in a volcano plot, including 416 upregulated genes (red dots) and 348 downregulated genes (green dots). **F** GO analyses exploring the cellular components, molecular functions, and biological processes in which DEGs were enriched were plotted based upon gene number, with darker blue dots indicating more significant enrichment. **G** KEGG enrichment signaling analysis results. * $P < 0.05$, ** $P < 0.01$, *** $P < 0.001$, **** $P < 0.0001$. Student's t-test. NC negative control, si small interfering RNA, DEGs different expression genes, GO gene ontology, KEGG kyoto encyclopedia of genes and genomes

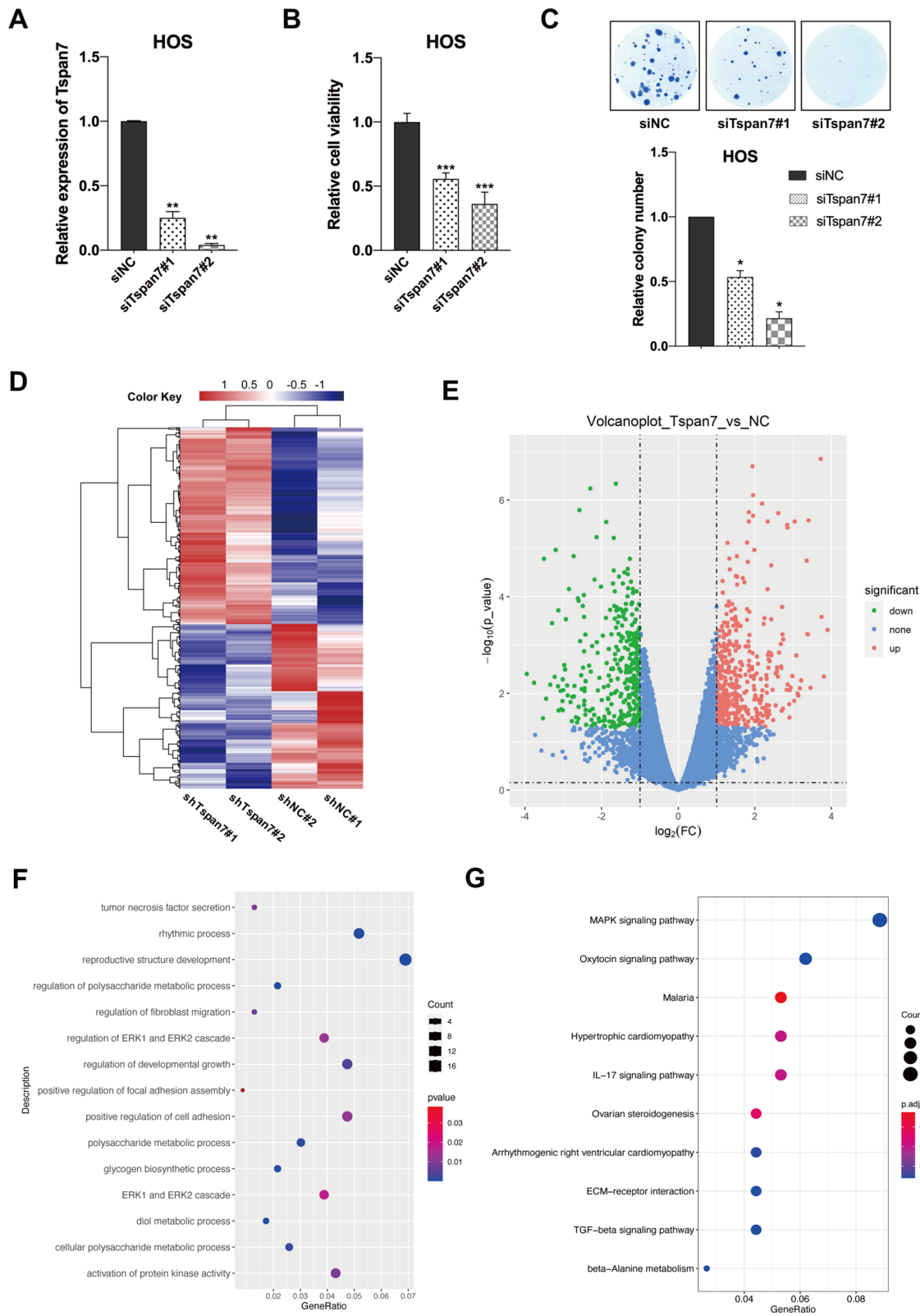


Fig. 2 (See legend on previous page.)

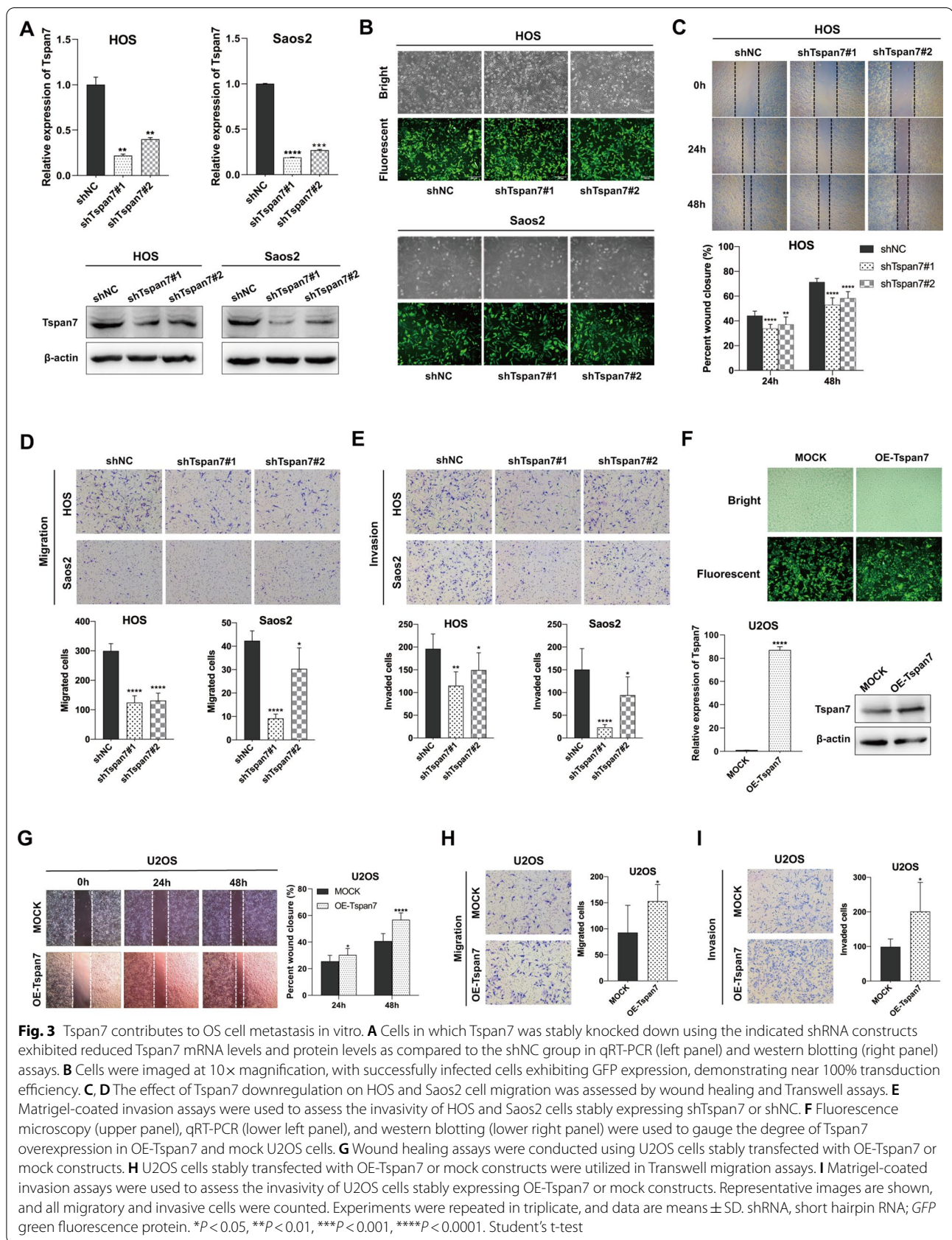


Fig. 3 Tspan7 contributes to OS cell metastasis in vitro. **A** Cells in which Tspan7 was stably knocked down using the indicated shRNA constructs exhibited reduced Tspan7 mRNA levels and protein levels as compared to the shNC group in qRT-PCR (left panel) and western blotting (right panel) assays. **B** Cells were imaged at 10× magnification, with successfully infected cells exhibiting GFP expression, demonstrating near 100% transduction efficiency. **C, D** The effect of Tspan7 downregulation on HOS and Saos2 cell migration was assessed by wound healing and Transwell assays. **E** Matrigel-coated invasion assays were used to assess the invasivity of HOS and Saos2 cells stably expressing shTspan7 or shNC. **F** Fluorescence microscopy (upper panel), qRT-PCR (lower left panel), and western blotting (lower right panel) were used to gauge the degree of Tspan7 overexpression in OE-Tspan7 and mock U2OS cells. **G** Wound healing assays were conducted using U2OS cells stably transfected with OE-Tspan7 or mock constructs. **H** U2OS cells stably transfected with OE-Tspan7 or mock constructs were utilized in Transwell migration assays. **I** Matrigel-coated invasion assays were used to assess the invasivity of U2OS cells stably expressing OE-Tspan7 or mock constructs. Representative images are shown, and all migratory and invasive cells were counted. Experiments were repeated in triplicate, and data are means ± SD. shRNA, short hairpin RNA; GFP green fluorescence protein. * $P < 0.05$, ** $P < 0.01$, *** $P < 0.001$, **** $P < 0.0001$. Student's t-test

group relative to the shNC group, and these results were further supported by histopathological analyses of lung sections following H&E staining (Fig. 4C–E). In addition, there was no obvious change in the body weight of the shTspan7-treated mice compared with the control group (Fig. 4F), whereas the lung weight of the shTspan7 group decreased slightly (Fig. 4G). Collectively, these data indicated that Tspan7 knockdown was sufficient to impair the *in vivo* metastatic ability of OS cells.

Tspan7 interacts with integrin $\beta 1$ to activate FAK-Src-Ras-ERK1/2 pathway

In order to induce signal transduction and thereby regulate cell functionality, tetraspanins form plasma membrane complexes with specific integrins. Mass spectrometry analyses indicated that Tspan7 was likely to interact with integrin $\beta 1$ (Additional file 1: Table S1). Subsequently, in co-IP assays, Tspan7 was confirmed to interact with integrin $\beta 1$ in OS cells (Fig. 5A). Western blotting analyses further indicated that Tspan7 knockdown resulted in reduced integrin $\beta 1$ protein levels in OS cells, whereas Tspan7 overexpression led to an increase in the expression of this integrin relative to the levels in control (Fig. 5B). These results demonstrated the interaction of Tspan7 and integrin $\beta 1$, suggesting that Tspan7 may govern OS metastatic progression through the signaling events downstream of integrin $\beta 1$.

FAK is the central mediator of canonical integrin-dependent signaling activity. Following ligand binding, integrins recruit FAK to their β subunit, leading to FAK Try397 autophosphorylation and subsequent association with Src. This leads to further kinase activation and the induction of downstream signaling such as the Ras-MAPK pathway and other signaling mechanisms. Ras-MAPK signaling downstream of FAK is facilitated by the generation of SH2 binding sites upon FAK autophosphorylation [35, 36]. Integrin $\beta 1$ interactions with FAK have reportedly been linked to pancreatic tumor metastatic progression through Ras and ERK1/2 signaling pathway activation [37]. To confirm the relationship between Tspan7 and integrin $\beta 1$ signaling in OS cells, we analyzed the protein levels of FAK, Src, Ras, and ERK1/2 in OS cell lines in which Tspan7 had been downregulated or upregulated (Fig. 5C, D). This experiment revealed that Tspan7 positively regulated the levels of p-FAK (Y397), p-FAK

(Y925), p-Src, Ras, and p-ERK1/2. To confirm a role for Tspan7 in the activation of these signaling pathways, U2OS cells overexpressing Tspan7 were treated with the Ras inhibitor Salirasib. Such treatment markedly suppressed ERK1/2 phosphorylation, which occurs downstream of Ras, in these cells (Fig. 5E). In addition, Ras inhibition was sufficient to impair the enhanced invasive and migratory activities of Tspan7 overexpressing cells as compared with untreated cells (Fig. 5F). In light of these results, it appears likely that Tspan7 can promote OS cell metastasis via forming a complex with $\beta 1$ integrin and thereby inducing FAK-Src-Ras-ERK1/2 pathway activation.

Discussion

This study is the first to our knowledge to have explored the mechanistic role of Tspan7 in OS. Although the combinations of surgery and chemotherapy afford positive outcomes to a large proportion of patients with this form of cancer, outcomes still remain unsatisfactory for those with recurrent, unresectable, or metastatic disease. It is thus critical that the biological basis for OS might be further elucidated to identify novel approaches to treat this debilitating disease. In the present study, we found that abrogation of Tspan7 resulted in the impaired proliferation of OS tumor cells relative to control cells, suggesting that Tspan7 may function as a key regulator of OS development and/or progression.

Through RNA-seq analyses, we sought to develop a more mechanistic understanding of how Tspan7 shapes OS cell biology. GO term analyses indicated that the DEGs upon Tspan7 knockdown were enriched for biological processes such as fibroblast migration, protein kinase activity, ERK1/2 signaling, developmental growth, and cell adhesion, all of which are central to metastatic progression. In total, we identified 416 upregulated and 348 downregulated genes among Tspan7 deleted OS cells, with FN1 being of particular interest in this context owing to its status as a mesenchymal marker of EMT associated with adhesion, migration, and invasion [38, 39]. These results thus supported a key role of Tspan7 in OS metastasis and underscored a likely link between this protein and EMT progress. Metastatic progression, particularly to the lung, is one of the primary causes of poor OS patient outcomes [40]. Early-stage cancer patients exhibit a 5 year survival rate of

(See figure on next page.)

Fig. 4 Tspan7 controls EMT induction, and knocking down of it suppresses *in vivo* OS metastasis. **A** Expression of EMT markers in HOS and U2OS cells stably knockdown or overexpression Tspan7. **B** Quantification of the western blotting results presented in **A**. **C** Representative images of lungs harboring OS metastases (arrows) on day 30 following the injection of HOS cells expressing shNC or shTspan7. **D** The presence of metastatic foci (dotted lines and black arrows) in lung pathological sections was assessed after H&E staining. Blue arrows indicate alveolar tissue. Scale bar = 40 μ m and 10 μ m. **E** Numbers of lung metastases per group were quantified (5 mice/group). **F** The administration of shTspan7 did not influence the body weights in the mice. **G** The administration of shTspan7 reduced slightly the lung weights in the mice. * $P < 0.05$, ** $P < 0.01$. Student's t-test

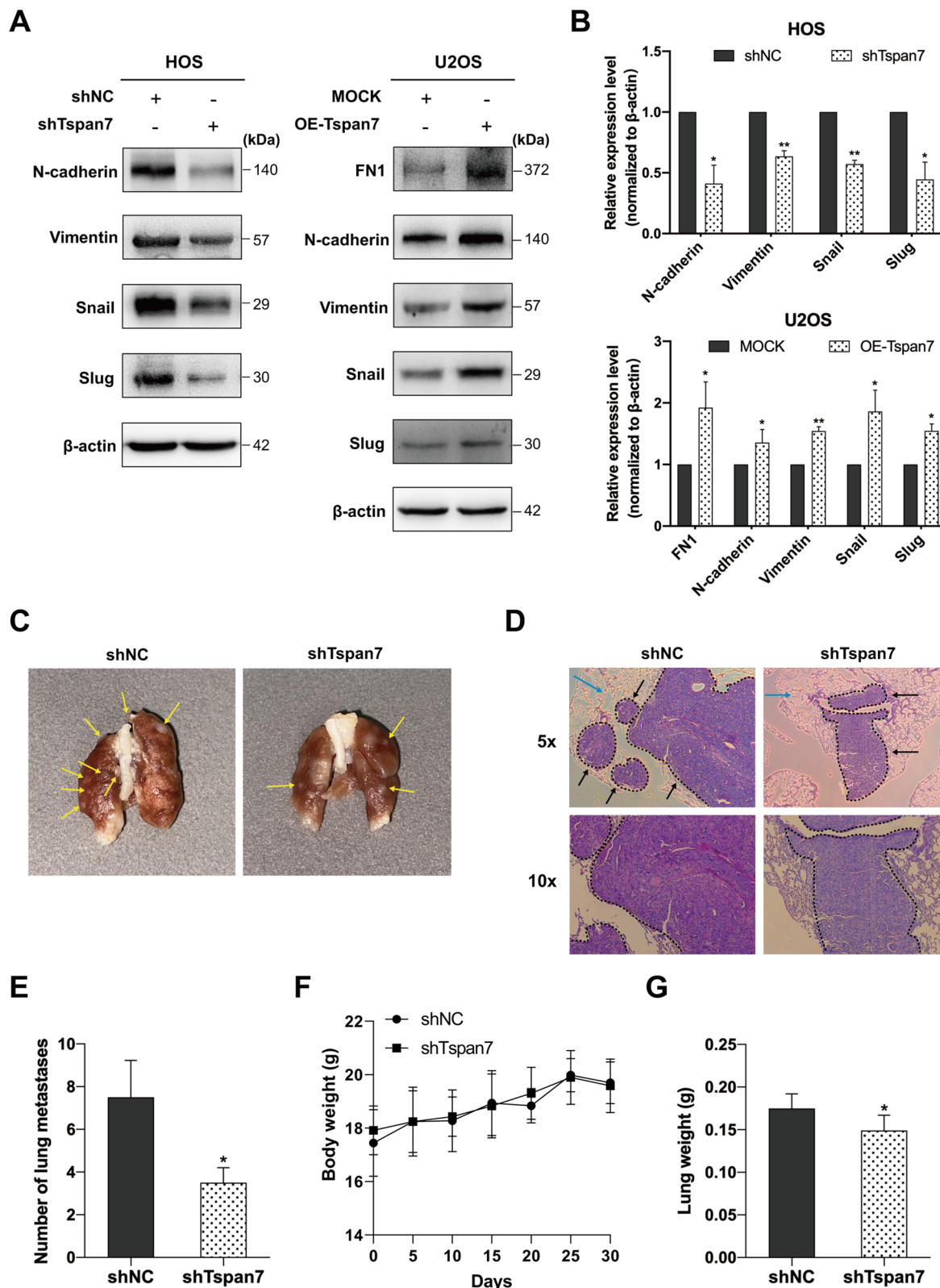


Fig. 4 (See legend on previous page.)

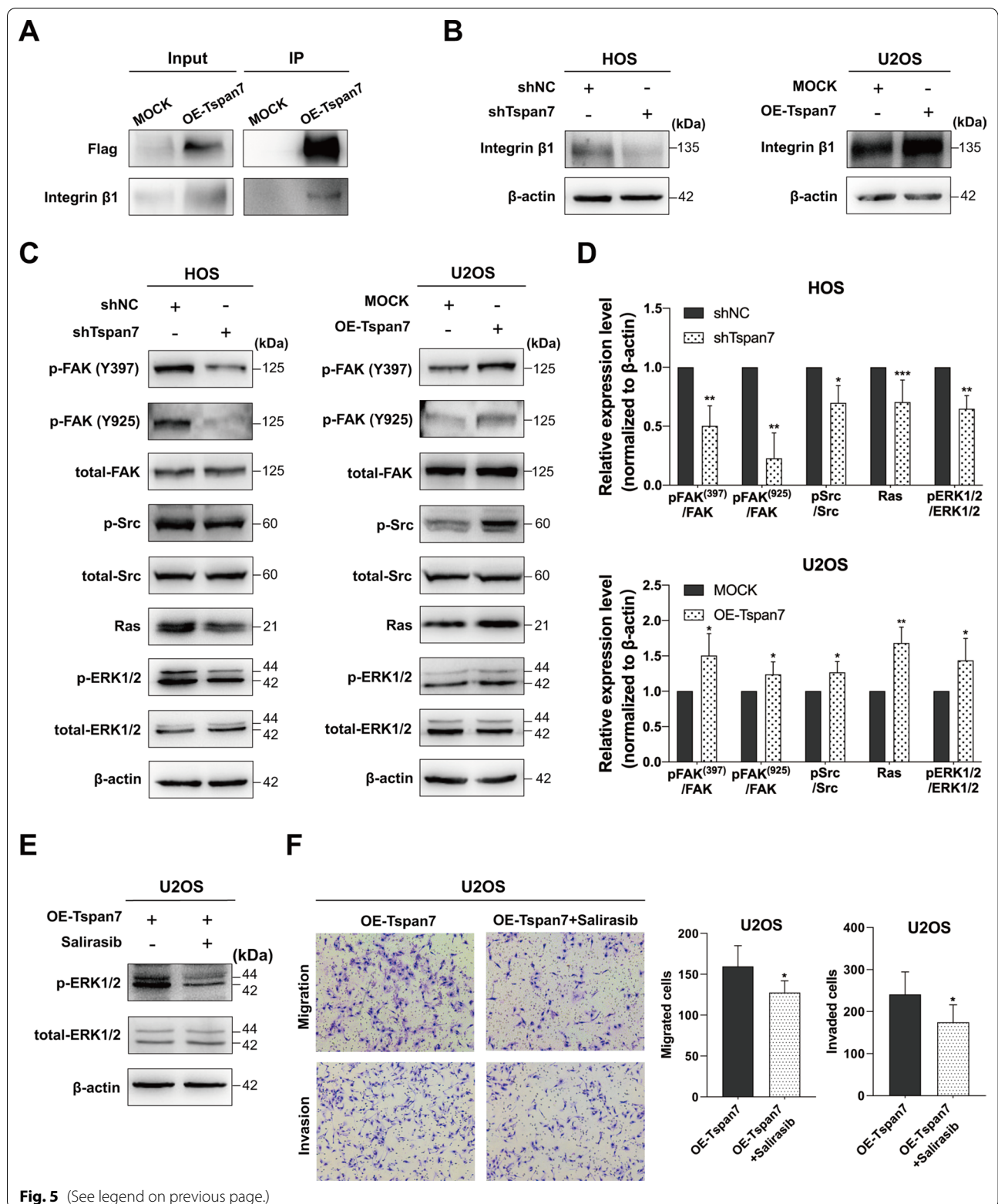
>50%, but this rate drops to <20% when tumors undergo metastasis via the lymphatic or circulatory systems [41], with such metastases being linked to 90% of cancer-associated mortality. The EMT is a dynamic and reversible process that facilitates the migration, dissemination, and metastatic growth of OS cells at distant tissue sites [42, 43], and EMT inhibition can thus suppress tumor metastasis. The EMT progression is characterized by the upregulation of the mesenchymal markers including FN1, N-cadherin, and Vimentin together with a loss of the epithelial markers E-cadherin and β -catenin [44]. Several transcription factors, such as Slug and Snail1, have also been identified as key regulators of OS cell invasion and metastasis owing to their ability to control the EMT process [45, 46]. The Wnt/ β -catenin, Ras/ERK, TGF- β , and PI3K-AKT pathways have also been shown to shape EMT induction in the oncogenic contexts [47–50]. To explore the functional importance of Tspan7 in this context, we knocked down or overexpressed this protein in OS cells and assessed their migration and invasion. Tspan7 knockdown in Saos2 and HOS cells markedly reduced the migratory and invasive activities of these cells, whereas its overexpression in U2OS cells had enhanced these capabilities. We also found that FN1 was upregulated in U2OS cells overexpressing Tspan7. Intriguingly, Tspan7 knockdown reduced the expression of markers consistent with EMT induction including N-cadherin, Vimentin, Snail1, and Slug, whereas the opposite effects were observed upon Tspan7 overexpression. Overall, these data suggested that Tspan7 can promote OS development by inducing EMT and thereby driving cellular migration and invasion.

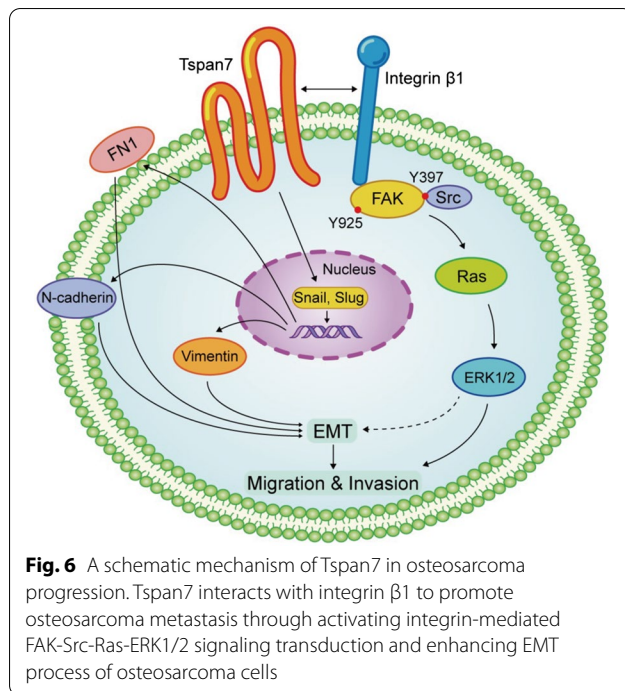
Changes in ECM interactions and adhesion molecule expression play central roles in EMT induction [51]. TM4SF proteins broadly regulate integrin-mediated cellular migration through the interactions with integrins, which are adhesion receptors that control the interactions between cells and ECM [52]. Lee et al. [10], for example, found that in prostate cancer cells, CD82 was able to interact with the $\alpha 3\beta 1/\alpha 5\beta 1$ integrins to suppress FAK/Src and integrin-linked kinase (ILK) signaling and thereby disrupted the EMT process. Conversely, the CD151- $\alpha 3\beta 1$ complex can synergize with EGFR to enhance glioblastoma cell metastasis via the activation of FAK^{Y397} and GTPase signaling pathways [53]. For the present study, we thus

primarily focused on key integrins which play a stimulatory role in the context of OS cell metastatic progression. Integrin $\beta 1$ was shown by Li et al. [54] to suppress the apoptotic death of OS cells and enhanced cell migration, while Jiang et al. [55] similarly found that integrin $\beta 1$ upregulation was linked to OS cell invasivity and EMT induction. Ren et al. [56] determined that integrin $\alpha v\beta 3$ was linked to OS cell metastasis through the induction of ERK1/2 signaling, and the interactions of tetraspanins and $\beta 1$ integrin have been shown to be key mediators of tumor cell metastasis [8]. $\beta 1$ integrin recruitment to ECM induced FAK^{Y397} autophosphorylation, which in turn facilitated Src-family kinase (SFK) recruitment and the subsequent phosphorylation of FAK at the Try407 and/or Try925 residues to trigger Ras-ERK signaling [57, 58]. In this research, through mass spectrometric analysis, we identified a series of potential Tspan7-interacting proteins in which integrin $\beta 1$ was particularly noteworthy. Next, we performed a co-IP assay and determined that Tspan7 and $\beta 1$ integrin directly interacted with each other. Interestingly, we found that the reduction of Tspan7 reduced integrin $\beta 1$ expression in protein levels, and Tspan7 overexpression promoted $\beta 1$ expression. Nevertheless, no change in mRNA level of integrin $\beta 1$ was observed according to our RNA-Seq analysis. The enhanced $\beta 1$ integrin protein expression without the alteration at the mRNA level suggests that Tspan7 may upregulate $\beta 1$ integrin at the posttranscriptional level. Although the mechanisms by which Tspan7 modulates $\beta 1$ integrin expression remain unknown, Tspan7 contributed to OS development depending on integrin-mediated downstream signaling pathway. Through a series of western blotting assays following Tspan7 transfection, we were able to detect a role for this tetraspanin in the FAK-Src-Ras-ERK1/2 signaling pathway, consistent with our RNA-seq data indicating the enrichment of Tspan7 in the regulation of ERK1/2 cascade (GO: 0,070,372). Lastly, we found that Ras inhibitor Salirasib was able to inhibit Tspan7 overexpression-induced ERK1/2 phosphorylation, migration and invasion in OS cells, implying the role of Tspan7 as a regulator of OS cell metastasis. Of note, because the Ras-ERK are vital regulators of EMT pathway [59], we hypothesized that Tspan7 regulated EMT process was ERK-dependent. As schemed in Fig. 6, Tspan7 may contribute to the metastatic progression of OS cell through interacting with $\beta 1$

(See figure on next page.)

Fig. 5 Tspan7 complexes with $\beta 1$ integrin to promote FAK-Src-Ras-ERK1/2 pathway activation. **A** Co-immunoprecipitation assays revealed interactions between Tspan7 and integrin $\beta 1$. **B** Integrin $\beta 1$ levels were assessed in HOS-shTspan7 and U2OS-Tspan7 cells via western blotting. **C** Proteins associated with the FAK-Src-Ras-ERK1/2 pathway (FAK, pFAK^{Y397}, pFAK^{Y925}, Ras, ERK1/2, and pERK1/2) were assessed by western blotting, with β -actin as a loading control. **D** Quantification of the western blotting results presented in **C**. **E** Signaling downstream of Ras in Tspan7-overexpressing U2OS cells treated with Salirasib (50 μ M) was assessed via western blotting. **F** U2OS-Tspan7 cells treated with or without Salirasib (50 μ M) were assessed by migration and invasion assays. Representative cell images are shown, and cells were counted. All experiments were repeated two or three times. * $P < 0.05$, ** $P < 0.01$, *** $P < 0.001$





integrin and subsequently activating FAK-Src-Ras-ERK1/2 pathway, thus resulting in EMT induction. Nevertheless, the mechanisms of whereby Tspan7 regulates the EMT process in OS cells require further exploration.

Conclusion

In summary, our data provide new evidence indicating that Tspan7 serves as a key oncogenic factor that drives OS cell proliferation, EMT induction, and metastasis in vitro and in vivo. Mechanistically, we find that Tspan7 is able to directly interact with β 1 integrin to augment FAK-Src-Ras-ERK1/2 signaling within OS cells so as to drive enhanced cell migration and invasion. As such, Tspan7 may represent a promising therapeutic target worthy amenable to pharmacological intervention aimed at improving OS patient outcomes.

Abbreviations

Tspan7: Tetraspanin-7; OS: Osteosarcoma; TM4SF: Transmembrane-4 superfamily; TEM: Tetraspanin-enriched microdomains; EMT: Epithelial to mesenchymal transition; OB: Osteoblast; MSC: Mesenchymal stem cell; qRT-PCR: Real-time quantitative polymerase chain reaction; WB: Western blot; IP: Immunoprecipitation; HE: Hematoxylin–eosin; GAPDH: Glyceraldehyde-3-phosphate dehydrogenase; SEM: Standard error of the mean; SD: Standard deviation; ROC: Receiver operating characteristic; AUC: Area under the curve; GFP: Green fluorescence protein; DEGs: Different expression genes; GO: Gene ontology; KEGG: Kyoto encyclopedia of genes and genomes.

Supplementary Information

The online version contains supplementary material available at <https://doi.org/10.1186/s12935-022-02591-1>.

Additional file 1: Identification of Tspan7-interacting proteins by mass spectrometry.

Acknowledgements

We would like to give our sincere appreciation to the reviewers for their helpful comments on this article. We thank Ms Chen Ding at the Second Hospital of Anhui Medical University for kind help in methodology.

Author contributions

YW and LP conceptualized the study. LG contributed to the data curation. JW conducted the formal analysis. SS, LW, and JW investigated the study. LT conducted the project administration. XY and JZ contributed to the methodology. SF conducted the visualization. SS wrote the original draft. SS and LP wrote, reviewed, and edited the manuscript. All authors read and approved the final manuscript.

Funding

This work was supported by the National Natural Science Foundation of China (Grant No. 81903661), and the Project of State Key Laboratory of Radiation Medicine and Protection of Soochow University (Grant No. GZK1202129).

Availability of data and materials

The original contributions presented in the study are included in the article. Further inquiries can be directed to the corresponding author.

Declarations

Ethics approval and consent to participate

The animal study was reviewed and approved by Ethics Committee of the Third Affiliated Hospital of Soochow University (Approval Number: 2021-006).

Consent for publication

Not applicable.

Competing interests

The authors declare that the research was conducted in the absence of any commercial or financial relationships that could be construed as a potential competing interest.

Received: 1 November 2021 Accepted: 18 April 2022

Published online: 06 May 2022

References

- Harting MT, Blakely ML. Management of osteosarcoma pulmonary metastases. *Semin Pediatr Surg.* 2006;15(1):25–9.
- Gorlick R, Khanna C. Osteosarcoma. *J Bone Miner Res.* 2010;25(4):683–91.
- Ferrari S, et al. The treatment of nonmetastatic high grade osteosarcoma of the extremity: review of the Italian Rizzoli experience. Impact on the future. *Cancer Treat Res.* 2009;152:275–87.
- Zhang B, et al. The efficacy and safety comparison of first-line chemotherapeutic agents (high-dose methotrexate, doxorubicin, cisplatin, and ifosfamide) for osteosarcoma: a network meta-analysis. *J Orthop Surg Res.* 2020;15(1):51.
- Beckwith KA, Byrd JC, Muthusamy N. Tetraspanins as therapeutic targets in hematological malignancy: a concise review. *Front Physiol.* 2015;6:91.

6. Luan M, et al. The peptide mimicking small extracellular loop domain of CD82 inhibits tumor cell migration, adhesion and induces apoptosis by inhibiting integrin mediated signaling. *Biochem Biophys Res Commun.* 2018;503(4):2206–11.
7. Claas C, Stipp CS, Hemler ME. Evaluation of prototype transmembrane 4 superfamily protein complexes and their relation to lipid rafts. *J Biol Chem.* 2001;276(11):7974–84.
8. Detchokul S, et al. Tetraspanins as regulators of the tumour microenvironment: implications for metastasis and therapeutic strategies. *Br J Pharmacol.* 2014;171(24):5462–90.
9. Wang X, et al. TSPAN7 promotes the migration and proliferation of lung cancer cells via epithelial-to-mesenchymal transition. *Oncotargets Ther.* 2018;11:8815–22.
10. Lee J, et al. The metastasis suppressor CD82/KAI1 inhibits fibronectin adhesion-induced epithelial-to-mesenchymal transition in prostate cancer cells by repressing the associated integrin signaling. *Oncotarget.* 2017;8(11):1641–54.
11. Yu Y, et al. CD151 promotes cell metastasis via activating TGF-beta1/Smad signaling in renal cell carcinoma. *Oncotarget.* 2018;9(17):13313–23.
12. Zhang HS, et al. TSPAN8 promotes colorectal cancer cell growth and migration in LSD1-dependent manner. *Life Sci.* 2020;241: 117114.
13. Lupia A, et al. CD63 tetraspanin is a negative driver of epithelial-to-mesenchymal transition in human melanoma cells. *J Invest Dermatol.* 2014;134(12):2947–56.
14. Sheng W, et al. Calreticulin promotes EGF-induced EMT in pancreatic cancer cells via integrin/EGFR-ERK/MAPK signaling pathway. *Cell Death Dis.* 2017;8(10): e3147.
15. Hynes RO. Integrins: bidirectional, allosteric signaling machines. *Cell.* 2002;110(6):673–87.
16. Pan L, et al. Research advances on structure and biological functions of integrins. *Springerplus.* 2016;5(1):1094.
17. Bassani S, Cingolani LA. Tetraspanins: interactions and interplay with integrins. *Int J Biochem Cell Biol.* 2012;44(5):703–8.
18. Hemler ME. Integrin associated proteins. *Curr Opin Cell Biol.* 1998;10(5):578–85.
19. Yu J, et al. The CD9, CD81, and CD151 EC2 domains bind to the classical RGD-binding site of integrin alphavbeta3. *Biochem J.* 2017;474(4):589–96.
20. Hosokawa Y, et al. Molecular cloning of a cDNA encoding mouse A15, a member of the transmembrane 4 superfamily, and its preferential expression in brain neurons. *Neurosci Res.* 1999;35(4):281–90.
21. Piliuso G, et al. Assessment of de novo copy-number variations in Italian patients with schizophrenia: detection of putative mutations involving regulatory enhancer elements. *World J Biol Psychiatry.* 2019;20(2):126–36.
22. Bassani S, Passafaro M. TSPAN7: a new player in excitatory synapse maturation and function. *BioArchitecture.* 2012;2(3):95–7.
23. Zemni R, et al. A new gene involved in X-linked mental retardation identified by analysis of an X;2 balanced translocation. *Nat Genet.* 2000;24(2):167–70.
24. Eugster A, et al. Cytoplasmic ends of tetraspanin 7 harbour epitopes recognised by autoantibodies in type 1 diabetes. *Diabetologia.* 2019;62(5):805–10.
25. Walther D, et al. Tetraspanin 7 autoantibodies in type 1 diabetes. *Diabetologia.* 2016;59(9):1973–6.
26. Cheong CM, et al. Tetraspanin 7 (TSPAN7) expression is upregulated in multiple myeloma patients and inhibits myeloma tumour development in vivo. *Exp Cell Res.* 2015;332(1):24–38.
27. Wuttig D, et al. CD31, EDNRB and TSPAN7 are promising prognostic markers in clear-cell renal cell carcinoma revealed by genome-wide expression analyses of primary tumors and metastases. *Int J Cancer.* 2012;131(5):E693-704.
28. Dumur CI, et al. Genes involved in radiation therapy response in head and neck cancers. *Laryngoscope.* 2009;119(1):91–101.
29. Davidson B, et al. Gene expression signatures of primary and metastatic uterine leiomyosarcoma. *Hum Pathol.* 2014;45(4):691–700.
30. Ito E, et al. A tetraspanin-family protein, T-cell acute lymphoblastic leukemia-associated antigen 1, is induced by the Ewing's sarcoma-Wilms' tumor 1 fusion protein of desmoplastic small round-cell tumor. *Am J Pathol.* 2003;163(6):2165–72.
31. Qi Y, et al. Expression and function of transmembrane 4 superfamily proteins in digestive system cancers. *Cancer Cell Int.* 2020;20:314.
32. Yu X, et al. TSPAN7 exerts anti-tumor effects in bladder cancer through the PTEN/PI3K/AKT pathway. *Front Oncol.* 2020;10: 613869.
33. Ordas L, et al. Mechanical control of cell migration by the metastasis suppressor tetraspanin CD82/KAI1. *Cells.* 2021;10(6):1545.
34. Zhang Z, et al. CD151 knockdown inhibits osteosarcoma metastasis through the GSK-3beta/beta-catenin/MMP9 pathway. *Oncol Rep.* 2016;35(3):1764–70.
35. Schlaepfer DD, et al. Integrin-mediated signal transduction linked to Ras pathway by GRB2 binding to focal adhesion kinase. *Nature.* 1994;372(6508):786–91.
36. Oktay M, et al. Integrin-mediated activation of focal adhesion kinase is required for signaling to Jun NH2-terminal kinase and progression through the G1 phase of the cell cycle. *J Cell Biol.* 1999;145(7):1461–9.
37. Sawai H, et al. Activation of focal adhesion kinase enhances the adhesion and invasion of pancreatic cancer cells via extracellular signal-regulated kinase-1/2 signaling pathway activation. *Mol Cancer.* 2005;4:37.
38. Cai X, et al. Down-regulation of FN1 inhibits colorectal carcinogenesis by suppressing proliferation, migration, and invasion. *J Cell Biochem.* 2018;119(6):4717–28.
39. Son H, Moon A. Epithelial-mesenchymal transition and cell invasion. *Toxicol Res.* 2010;26(4):245–52.
40. Guo J, et al. Dynamic contrast-enhanced magnetic resonance imaging as a prognostic factor in predicting event-free and overall survival in pediatric patients with osteosarcoma. *Cancer.* 2012;118(15):3776–85.
41. Donohoe J, et al. Predicting late-stage breast cancer diagnosis and receipt of adjuvant therapy: applying current spatial access to care methods in Appalachia. *Med Care.* 2015;53(11):980–8.
42. Shen S, et al. A miR-135b-TAZ positive feedback loop promotes epithelial-mesenchymal transition (EMT) and tumorigenesis in osteosarcoma. *Cancer Lett.* 2017;407:32–44.
43. Lu KH, et al. 3-Hydroxyflavone inhibits human osteosarcoma U2OS and 143B cells metastasis by affecting EMT and repressing u-PA/MMP-2 via FAK-Src to MEK/ERK and RhoA/MLC2 pathways and reduces 143B tumor growth in vivo. *Food Chem Toxicol.* 2016;97:177–86.
44. Campbell K. Contribution of epithelial-mesenchymal transitions to organogenesis and cancer metastasis. *Curr Opin Cell Biol.* 2018;55:30–5.
45. Yang G, Yuan J, Li K. EMT transcription factors: implication in osteosarcoma. *Med Oncol.* 2013;30(4):697.
46. Yu X, Yustein JT, Xu J. Research models and mesenchymal/epithelial plasticity of osteosarcoma. *Cell Biosci.* 2021;11(1):94.
47. Ding Q, et al. LncRNA CRNDE is activated by SP1 and promotes osteosarcoma proliferation, invasion, and epithelial-mesenchymal transition via Wnt/beta-catenin signaling pathway. *J Cell Biochem.* 2020;121(5–6):3358–71.
48. Qiu XY, et al. PD-L1 confers glioblastoma multiforme malignancy via Ras binding and Ras/Erk/EMT activation. *Biochim Biophys Acta Mol Basis Dis.* 2018;1864(5):1754–69.
49. Wang J, Liang S, Duan X. Molecular mechanism of miR-153 inhibiting migration, invasion and epithelial-mesenchymal transition of breast cancer by regulating transforming growth factor beta (TGF-beta) signaling pathway. *J Cell Biochem.* 2019;120(6):9539–46.
50. Wei R, et al. FAT4 regulates the EMT and autophagy in colorectal cancer cells in part via the PI3K-AKT signaling axis. *J Exp Clin Cancer Res.* 2019;38(1):112.
51. Zeisberg M, Neilson EG. Biomarkers for epithelial-mesenchymal transitions. *J Clin Invest.* 2009;119(6):1429–37.
52. Berditchevski F. Complexes of tetraspanins with integrins: more than meets the eye. *J Cell Sci.* 2001;114(Pt 23):4143–51.
53. Zhou P, et al. CD151-alpha3beta1 integrin complexes are prognostic markers of glioblastoma and cooperate with EGFR to drive tumor cell motility and invasion. *Oncotarget.* 2015;6(30):29675–93.
54. Li R, et al. NF-kappaB signaling and integrin-beta1 inhibition attenuates osteosarcoma metastasis via increased cell apoptosis. *Int J Biol Macromol.* 2019;123:1035–43.

55. Jiang Y, Luo Y. LINC01354 promotes osteosarcoma cell invasion by up-regulating Integrin beta1. *Arch Med Res.* 2020;51(2):115–23.
56. Ren P, et al. Serum amyloid A promotes osteosarcoma invasion via upregulating alphavbeta3 integrin. *Mol Med Rep.* 2014;10(6):3106–12.
57. Mitra SK, Schlaepfer DD. Integrin-regulated FAK-Src signaling in normal and cancer cells. *Curr Opin Cell Biol.* 2006;18(5):516–23.
58. Qi Y, et al. TSPAN9 and EMILIN1 synergistically inhibit the migration and invasion of gastric cancer cells by increasing TSPAN9 expression. *BMC Cancer.* 2019;19(1):630.
59. Lamouille S, Xu J, Derynck R. Molecular mechanisms of epithelial-mesenchymal transition. *Nat Rev Mol Cell Biol.* 2014;15(3):178–96.

Publisher's Note

Springer Nature remains neutral with regard to jurisdictional claims in published maps and institutional affiliations.

Ready to submit your research? Choose BMC and benefit from:

- fast, convenient online submission
- thorough peer review by experienced researchers in your field
- rapid publication on acceptance
- support for research data, including large and complex data types
- gold Open Access which fosters wider collaboration and increased citations
- maximum visibility for your research: over 100M website views per year

At BMC, research is always in progress.

Learn more biomedcentral.com/submissions

